M phase phosphoprotein 1 is a human plus-end-directed kinesin-related protein required for cytokinesis

Abaza Aouatef [1] , Soleilhac Jean-Marc [1] , Westendorf Joanne [1] , Piel Matthieu [2] , Crevel Isabelle [3] , Roux Aurelien [4] , Pirollet Fabienne [1 *]

[1] Organisation Fonctionnelle du Cytosquelette INSERM : U366, Université Joseph Fourier - Grenoble I, Cea LYON 17, Rue Des Martyrs 38054 Grenoble Cedex 9,FR

[2] CDC, Compartimentation et dynamique cellulaires CNRS : UMR144, Institut Curie, 26 Rue d'Ulm 75248 Paris Cedex 05,FR

[3] Marie Curie Research Institute MRCI, Oxford,GB

[4] UPCC, Unite physico-chimie Curie CNRS : UMR168, Institut Curie, Bâtiment Curie 26 rue d'Ulm 75248 Paris Cedex 05,FR

* Correspondence should be adressed to: Fabienne Pirollet <Fabienne.Pirollet@ujf-grenoble.fr>

A. A. and J-M. S. contributed equally to this work

Abstract
Summary

The human M-Phase Phosphoprotein 1 (MPP1), previously identified through a screening of a subset of proteins specifically phosphorylated at the G2/M transition (1), is characterized as a plus-end-directed kinesin-related protein. Recombinant MPP1 exhibits in vitro microtubule-binding and microtubule-bundling properties as well as microtubules-stimulated ATPase activity. In gliding experiments using polarity-marked microtubules, MPP1 is a slow molecular motor that moves towards the microtubule plus-end at a 0.07 m/s speed. In cycling cells, MPP1 localizes mainly to the nuclei in interphase. During mitosis, MPP1 is diffuse throughout the cytoplasm in metaphase and subsequently localizes to the midzone to further concentrate on the midbody. MPP1 suppression by RNA interference induces failure of cell division late in cytokinesis. We conclude that MPP1 is a new mitotic molecular motor required for completion of cytokinesis.

MESH Keywords Adenosine Triphosphatases ; metabolism ; Amino Acid Sequence ; Animals ; Cell Cycle Proteins ; Cell Division ; physiology ; Cell Line ; Cell Movement ; Cells ; Cultured ; Cloning ; Molecular ; Cytoplasm ; metabolism ; DNA ; Complementary ; metabolism ; Electrophoresis ; Polyacrylamide Gel ; Epitopes ; Flow Cytometry ; G2 Phase ; Gene Library ; Genome ; Green Fluorescent Proteins ; Hela Cells ; Humans ; Immunoblotting ; Insects ; Kinesin ; metabolism ; Kinetics ; Luminescent Proteins ; metabolism ; Metaphase ; Microscopy ; Fluorescence ; Microtubules ; metabolism ; Mitosis ; Molecular Sequence Data ; Mutagenesis ; Site-Directed ; Phosphoproteins ; metabolism ; physiology ; Phosphorylation ; Protein Structure ; Tertiary ; RNA Interference ; RNA ; Small Interfering ; metabolism ; Recombinant Fusion Proteins ; metabolism ; Recombinant Proteins ; metabolism ; Sequence Analysis ; DNA ; Sequence Homology ; Amino Acid ; Time Factors ; Tissue Distribution ; Transfection

Introduction

Eukaryotic cells exhibit dramatic changes of microtubule organization and dynamics as they enter mitosis (2,3). These changes are timely and spatially coordinated with nucleus and membranes alterations by the tight control of M-phase promoting factor (MPF)1, whose catalytic component, the $p34^{cdc2}$ or cdk1 kinase becomes activated at the G2-M transition (4,5). Extensive progress has been made to describe the complex circuitry of phosphatases and kinases, which regulates cdk1 activation (6,7) and the downstream molecular pathways (8,9).

Microtubule dynamics are an intrinsic property of the polymer of tubulin and are highly regulated by the balance of the activity of different factors throughout the cell cycle (10–12). Several Microtubule-Associated Proteins (MAPs) have been described to promote tubulin assembly and polymer stabilization or destabilization (13,14). Besides their roles in intracellular trafficking of organelles and vesicles during interphase, dyneins and Kinesin-Related Proteins (KRPs), microtubule-based molecular motors, play important roles in cell division. At each stage of mitosis or meiosis, dyneins and various KRPs interact with microtubules in order to insure centrosome separation, spindle formation and maintenance, chromosome congression and cytokinesis completion (15–19).

However, whereas it is well established that the $p34^{cdc2}$ kinase is centrally involved in the regulation of microtubule dynamics during mitosis (20), only a few cdc2 substrates with plausible involvement in the control of microtubule dynamics have been identified so far. The $p34^{cdc2}$ kinase phosphorylates the ubiquitous MAP4 during M-phase (21) and this phosphorylation abolishes MAP4 microtubule stabilizing activity (22). There is evidence that the phosphorylation of the microtubule destabilizing protein Stathmin/Op18 by $p34^{cdc2}$ is important for mitotic progression (23). Similar phosphorylation of the mitotic KRP Eg5 is required for Eg5-dependent centrosome migration and bipolar spindle formation in vivo (17). These data suggest that mitotic kinases regulate microtubule dynamics and organization by phosphorylating various microtubule-interacting proteins and this has been an incentive for the systematic search of mitotic phosphoproteins.

We have recently identified a subset of M-phase phosphoproteins by expression library screening using the MPM2 monoclonal antibody, which recognizes a phosphoepitope present on a set of 40 to 50 proteins that become phosphorylated at the G2-M transition (1,24–26). Among the 11 proteins identified, we show here that M-Phase Phosphoprotein 1 (MPP1) has extensive homology with proteins of the kinesin superfamily. We demonstrate that MPP1 is a plus-end directed molecular motor with an important role in cytokinesis.

Experimental procedures

Cloning and sequencing of full-length human MPP1 cDNA

Human MPP1 cDNAs were obtained by screening two λzapII cDNA libraries made from HeLa, one a generous gift from P. Chambon, the other a Uni-ZAP XR library from Stratagene, following standard procedures (27). Starting with the 645 bp N-terminal fragment of the previously described partial-length MPP1 cDNA 6-1 (24) as a probe, the human MPP1 cDNA, 1L9 (4265 bp) was isolated. The overlapping MPP1 cDNA, 1C12 (2822 bp) was obtained by a second round of screening using a N-terminal fragment of pBS-1L9. Full-length MPP1 plasmid, pBS-MPP1, was obtained by subcloning the 2408 bp N-terminal fragment of the pBS-1C12 in pBS-1L9. The HsMPP1 sequences are available under accession numbers AY282406, AY282407. Sequencing was performed by the Genome Express Company, Grenoble. The sequences were analyzed and database searches were performed with GCG, FASTA, BLAST programs available at NCBI or INFOBIOGEN ressources. Specific motifs were searched using PESTFIND, COIL, PredictNLS, pSORT programs.

FLAG epitope tagging of MPP1 by mutagenesis

The MPP1 coding sequence starting at base 70 was tagged using mutagenesis technique based on M13-phage ssDNA protocol (Amersham Sculptor Kit). 1C12 ssDNA was obtained using standard procedures (27). A 66-mer oligonucleotide was designed that introduced between bases 69–70, 36 bp containing a NotI restriction site and encoding MDYKDDDDK amino acids which correspond to the FLAG epitope upstream of the cleavage sequence of enterokinase. After sequencing of the 5′ end of a selected clone, the 3′ end fragment NsiI-BamHI (2484 bp) was replaced by the similar fragment obtained from the original 1C12 to ensure that no other mutations were introduced in plasmid pBS-m1C12. Orientation of the mutated Nterminal EcoRI fragment (484 bp) was inverted in the pBluescript vector and the 5145 bp NsiI fragment of pBS-MPP1 was subcloned into this plasmid to construct pBS-mMPP1 which encoded full-length MPP1 tagged with the FLAG epitope.

Expression and purification of recombinant MPP1 mutants in insects cells

A recombinant full-length MPP1 (rMPP1) and a truncated form (rMC1), both tagged with a N-terminal FLAG epitope, were produced by baculovirus expression following the manufacturer's instructions of the Bac-to-Bac system (Life Technologies). The mutated NotIKpnI fragment of pBS-mMPP1 and the NotI-XhoI of pBS-m1C12 were respectively subcloned into the pFastBac HTb vector in phase with its 6His coding sequence to generate doubly tagged recombinant viruses in Sf9 cells. Recombinant proteins were then expressed in High-Five cells, a generous gift of Dr B. Goud. Cells were harvested at 48 h after viral infection at MOI=2, frozen in liquid nitrogen and stored at −80°C. Frozen cell pellets were resuspended in ice-cold lysis buffer (50 mM Tris, pH=8, 0.5 M NaCl, 2 mM $MgCl_2$, 5 mM $CaCl_2$, 1 mM DTT, 0.02%(v/v) Triton X-100, in presence of Complete™ inhibitors (Boehringer). After sonication, the lysate was cleared by centrifugation at 90,000 g for 45 min at 4°C and loaded onto an Anti-FLAG M2-agarose column (Sigma). After washing, the adsorbed proteins were eluted with 3.5 M MgCl2 and buffer exchanged on a PD-10 column (Pharmacia) equilibrated in 50 mM Tris, pH=7.4, 0.2M NaCl. For biochemical studies, the 6His tag, which induces protein precipitation, was removed by cleavage with the TEV protease as described in the technical information (Life Technologies). The rMPP1 and rMC1 proteins were then concentrated on Ultrafree-4 centrifugal filters (Millipore). The final fractions were aliquoted, frozen in liquid nitrogen and stored at −80°C. For gliding assays, the proteins were complemented with 1 mM ATP, 2 mM $MgCl_2$, 0.1mg/ml casein and frozen without concentration. Protein concentration was determined colorimetrically using BSA as a standard and Bio-Rad Protein Assay (Bio-Rad).

Anti-MPP1 antibody production and purification

A polyclonal anti-MPP1 antibody was raised by Eurogentec using four injections of 100 μg of 6His-rMPP1 proteins in rabbit. The antibody was affinity-purified by three-step positive-negative affinity purification. The antiserum was filtered through 6His-FLAG-unrelated protein and 6His-rMC1 affinity-columns in order to remove any antibodies reacting with tags and conserved motifs present in the MPP1 motor domain. Specific anti-MPP1 antibody, which recognizes epitopes present in the C2 to tail domains, was then purified by passage of the filtrate onto a 6His-rMPP1-affinity column. Purified anti-MPP1 antibody was eluted with Tris 50 mM, $MgCl_2$ 3.5 M, pH=7.5, dialyzed overnight against PBS and stored at 4°C.

Fluorescent microtubule spindown assay

Purification of bovine brain tubulin (28), polymerisation and purification on glycerol cushion of taxol-stabilized microtubules (MTs) were performed using standard procedures. MTs concentration (i. e., concentration of tubulin dimer in MT polymer) was determined according to Desai et al (29). Recombinant MPP1 proteins, routinely 0.1 μM, were cleared by ultracentrifugation and mixed with taxol-MTs (1 μM) in 100 μ l BRB80 buffer supplemented with 10 μM taxol. After incubation for 15 min at 25°C, reaction was fixed with 1ml of MEM-50% sucrose containing 1% glutaraldehyde. MTs were diluted and sedimented through a glycerol cushion onto coverslips as described in (30). Coverslips were post-fixed in −20°C methanol for 6 min and washed three times for 10 min in PBS containing 0.1% NaBH4 to prevent glutaraldehyde autofluorescence. MTs and recombinant proteins were stained with rabbit anti-Glu and Δ2 tubulin antibodies (1/1,000; a generous gift of Dr D. Job (31) and a mouse anti-Flag M2 antibody (1/500, Sigma). Fluorescent labeling was performed with Alexa 488-labeled anti-rabbit (1/4,000) and TRITC-labeled anti-mouse (1/1,000) IgGs antibodies from Molecular Probes and Jackson.

Measurement of steady state ATPase rates

Steady-state MT-activated ATPase rates were measured using a pyruvate kinase/lactate dehydrogenase-linked assay, mainly as described in (32). Briefly, ATPase activities were assayed at 30°C in 1 ml reaction volume of 100 mM K-Pipes, pH=6.8, 4 mM $MgCl_2$, 1 mM EGTA, 1 mM PEP, 0.3 mM NADH, 40 U of pyruvate kinase and 55 U of lactate dehydrogenase. NADH oxidation was followed at 340 nm in a temperature-controlled UVIKON 923 spectrophotometer. Rates were determined during the linear phase after 5 min for attainment of steady state, using ε-NADH = 6220 $M^{-1}.cm^{-1}$. The kinetic parameters k_{cat}, $K_{1/2\ MT}$ (the concentration of MTs required for half-maximal activation) and Km for ATP were obtained by least squares fitting the MT activation or ATP dependent data to rectangular hyperbolae using Sigmaplot.

Motility assay with polarity-marked microtubules

A standard motility assay (33) was performed with recombinant MPP1 proteins using the fluorescence based kinesin motility kit from Cytoskeleton. Polarity marked MTs with a bright seed and a dim elongated segment at their plus-end were prepared by inclusion of NEM-treated tubulin, according to previously described protocols (see Methods page at the kinesin website http://www.proweb.org/kinesin). Briefly, acid-washed flow cells were coated with motor protein (typically 0.15 and 0.3 μM for rMPP1 and rMC1 respectively) in motility assay buffer (MAB = BRB80 buffer supplemented with 0.1 mg/ml casein, 1 mM ATP, 20 μM taxol and an oxygen scavenging mix). After 5 minutes at room temperature, non-adsorbed motor was washed out with two flow cell volumes of MAB. Asymmetrically labeled MTs (0.2 μM) were then flowed through the cell and allowed to interact with the motor for 5 minutes at room temperature. Finally, unbound MTs were washed out with 2 flow cell volumes of MAB. Video images of MTs were acquired in a thermostated room with a Princeton CCD Micromax RTE 1317K1 camera on a Zeiss Axioscop with a 100 × 1.3 NA Plan-Neofluar lens using IPLab software (Ropper Scientific). Measurement of MT velocities was performed using the RETRAC program available at http://mc11.mcri.ac.uk.

Preparation of a GFP fused mutant of MPP1

The 70–981 bp portion of MPP1 cDNA was amplified by recombinant PCR using TA-cloning kit (Invitrogen). This fragment was cloned into the XhoI site of pEGFP-C2 eukaryotic expression vector (Clontech), using an XhoI restriction site introduced upstream of the initiation codon. The pEGFP-sM plasmid obtained encodes the GFP protein fused to the N-terminus region of MPP1 extending from aa 1 to aa 304. The C-terminal HindIII-KpnI fragment of pBS-MPP1 was subcloned into this plasmid to construct pEGFP-MPP1-FL, which encodes the full-length fusion protein GFP-MPP1.

Cell culture and cloning

HeLa and HCT116 cells were grown in RPMI-1640 and McCoy medium (Gibco) supplemented with 10% FCS, respectively. HeLa cells were transfected with the various pEGFP-MPP1 plasmids using the FuGENE™ 6 transfection reagent as described by the manufacturer (Boehringer Mannheim). Stable clones expressing the GFP-MPP1-FL fusion protein were then isolated, by using the limited dilution method in the presence of 500 μg/ml G418. In some instances, cells were analyzed with treatment with 250 nM of trichostatin A overnight to increase expression (34).

SiRNA preparation and transfection

MPP1-specific small interfering RNA (siRNA) duplexes were designed according to Harborth et al (35). Sequences of the type $AA(N_{19})UU$ (N, any nucleotide) were searched in the open reading frame of MPP1-mRNA and submitted to a BLAST search to ensure their specificity. Selected 21-nt sense and 21-nt antisense oligonucleotides targeting MPP1 from position 424–446 (siRNA1) or 4782–4804 (siRNA2) relative to the start codon were purchased from Dharmacon (Lafayette, CO) in deprotected and desalted form. As unspecific siRNA controls, we used an unrelated sequence that failed to target p160ROCK mRNA (siRNAU) (36) or a siRNA1 sequence mutated on two nucleotides (siRNA1m). Annealing and transfection was performed as previously described (37). HCT116 cells were transfected with siRNAs

using Oligofectamine (InVitrogen). Mock-transfections were also performed using control buffer instead of oligonucleotides. At different time points after transfection, cells were harvested and either fixed and processed for FACS analyzis or analyzed by Western blot after addition of SDS-PAGE sample buffer. Time-lapse imaging was also performed.

Immunofluorescence microscopy

Exponentially growing cells were plated on glass coverslips and incubated for 24–36 hours. Cells were fixed in methanol at −20°C for 8 min and processed with primary and secondary antibodies diluted in PBS with 1mg/ml bovine serum albumin. The primary antibodies used were purified anti-MPP1 IgGs (5 μg/ml, this study), a mouse monoclonal anti β-tubulin 2–3 B11 (1/5,000, a generous gift of Drs A. Giraudel and L. Lafanechère, unpublished results) or mouse monoclonal anti-mitosin 14C10 (1 μg/ml, from GeneTex). Suitable Cy3- (Jackson, 1/1,000) or Alexa 488- (Molecular Probes, 1/500) conjugated antibodies were applied as secondary antibodies. DNA was stained with Hoechst 33258 (1 μg/ml) or Topro 3 (1/1,500, Molecular Probes). The coverslips were examined on a Zeiss microscope by using a 100 × 1.4 oil immersion objective. Confocal images were obtained on a TCS-SP2 Leica laser scanning microscope. Z series were collected and displayed images correspond to projections of optical sections (0.2 μm thick), which number varied in relation to the cell depth.

Flow cytometric analysis

For standard analysis of DNA content, cells were washed once with PBS, trypsinized, fixed with 4% paraformaldehyde in PBS for 10 min and permeabilized with 0.2% triton X-100 in PBS. DNA was stained overnight at 4°C with 2 μg/ml of Hoechst. Cells were sorted on a FACS Star Plus cytometer (Beckton and Dickinson Co). After collection of 20, 000 events, results were analyzed with CellQuest software and aggregated cells were gated out. For double staining of DNA and specific antigen, cells were fixed with ice-cold 70% ethanol. Labelling of MPP1 or mitosin was performed before the DNA counterstaining step by incubation with anti-MPP1 or anti-mitosin antibodies followed by Alexa 488-conjugated antirabbit or anti-mouse IgGs (1/500, Molecular Probes).

Time-lapse imaging

For phase-contrast imaging, control or MPP1 siRNA transfected cells were trypsinized 6 h after transfection and transferred into a multiple well chamber of a poly-dimethyl siloxane gel fixed on a glass chamber coated with collagen and fibronectin. Sequential phase-contrast images of the various samples were recorded on a Leica DMIRBE microscope controlled by Metamorph software (Universal Imaging) for 66 h. The microscope was equipped with an open chamber equilibrated in 5% CO_2 and maintained at 37°C, and images were taken with a 20x objective using a cooled MicroMax 1MHz CCD camera (Roper Scientific).

For GFP-MPP1 imaging during mitosis, stably transfected cells were plated on coated coverslips and maintained at 37°C in sealed chambers containing complete phenol red-free RPMI medium supplemented with 20 mM Hepes. Rounded cells were searched and time lapse Z-sequences were collected as described by Savino et al (38) on a Leica DMIRBE microscope controlled by Metamorph software (Universal Imaging). This microscope was equipped with a piezoelectric device for rapid and reproducible focal changes, a 100 × 1.4 NA Plan Apo lens, a cooled CCD camera (Micromax 5MHz; Roper Scientific) and a DG4 illumination device. Z-stacks were deconvoluted and maximal-intensity projections were constructed.

Results

Identification of MPP1 as a kinesin related protein present in several human tissues

The entire human MPP1 cDNA (6325 bp) was cloned using two rounds of conventional cDNA library screening, starting with the previously obtained partial clone 6-1 (24). Sequence comparison in databases showed that MPP1 belongs to the kinesin superfamily of motor proteins with the characteristic organization into three domains (15), as detailed in Fig 1A. A search of genome resources indicated that a unique human MPP1 gene located on chromosome 10 in the 10q23.31 region spreads at least 73 kb and consists of 33 exons. A mouse ortholog (82% similarity) encoded by a conserved syntheny was found on murine chromosome 19. Alignment of the conserved motor domains of MPP1 and conventional kinesin heavy chain, KHC (Fig 1B) showed that MPP1 motor exhibits two large insertions (186–263, 480–507), which span respectively between alpha helix 2 and β sheet 4 and alpha helix 6 and β sheet 9 when compared to KHC structural data (39,40).

For immunoblot analysis of MPP1 distribution, we used an affinity-purified MPP1 antibody directed against the C2 to tail domains (aa 651 to 1780) of MPP1 (Fig 2). This antibody reacted with a single 200 kDa band in HeLa cell extracts (Fig 2B, lane 3), which co-migrates with purified recombinant full-length MPP1 (Fig 2A and 2B, lane 1). MPP1 was detected in several human tissues, including brain, ovary and kidney (Fig 2B). In the testis extract, a strong signal corresponding to a slightly lower MW band was detected and may correspond to a testis specific splicing variant of MPP1.

Recombinant MPP1 behaves as a genuine molecular motor

To assay MPP1 motor activity, we used recombinant proteins corresponding either to the complete MPP1 (rMPP1) or to a deletion mutant of the protein containing the putative motor domain and the first α-helical domain (rMC1, Fig 2A). The proteins were assayed for the characteristic activities of genuine KRP i.e. regulated ATPase activity, binding to MTs and ability to induce microtubule gliding on motor coated coverslips (15,41) (Fig 3). Both rMPP1 and rMC1 exhibited a basal ATPase activity, which was activated by addition of MTs (~ 280 or 630-fold for rMPP1 and rMC1, respectively; Fig 3A). The k_{cat} and KmATP values of rMPP1 and rMC1 were close to each other and the MT concentration required for halfmaximal activation was ~6-fold higher for rMC1 mutant than for rMPP1.

The microtubule binding activity of rMPP1 and rMC1 could not be assayed by conventional MT pelleting assays (42) due to partial insolubility of the unbound proteins. For visualisation of microtubule binding, control microtubules or microtubules incubated with rMPP1 or with rMC1 were centrifuged on coverslips and subsequently double stained with tubulin and FLAG antibodies (Fig 3B). In control samples short individual MTs were observed. Incubation with rMPP1 or rMC1 prior to centrifugation induced extensive MTs cross-linking. Recombinant proteins were associated with microtubule bundles, while being undetectable on single polymers. When ATP was added in the incubation medium, microtubule bundling was inhibited in a dose dependent way and many individual MTs could be observed on the coverslip (Figure 3B and data not shown). These results indicate that both rMPP1 and rMC1 bind to MTs in an ATP-dependent way and induce microtubule bundling, in vitro.

To test the force-producing capability of MPP1, we used a multiple-motor assay using polarity-marked MTs. Protein rMC1 induced MT motility with the minus end leading and most of the MTs (>90%) were seen gliding (Fig 3C). MT gliding was also observed with rMPP1 but, curiously, only a subset of relatively short microtubules (1–5 μm in length) was seen moving (data not shown). In both cases, gliding was abolished in the presence of 1 mM AMP-PNP (data not shown). The average velocity of microtubule gliding was 0.07 ± 0.01 μm/s and 0.071 ± 0.007 μm/s for rMPP1 and rMC1, respectively. These data demonstrate that MPP1 is a slow plus-end directed KRP, when compared to already described motors (43).

MPP1 distribution during the cell cycle

MPP1 expression and localization during the cell cycle was investigated by immunofluorescence analysis of fixed HeLa cells (Fig 4). In interphase cells double stained with MPP1/tubulin antibodies, MPP1 was mainly localized in the nucleus. MPP1 was also detected in the cytoplasm as a punctuated pattern without clear association with microtubules (Fig 4A). The nuclear staining varied from cell to cell, suggesting a cell cycle dependent expression of the protein MPP1. This possibility was tested using indirect immunofluorescence and FACS analysis of HeLa cells double stained for MPP1 and mitosin, a centromere-associated-protein whose expression is strongly enhanced in G2 cells (44), (Fig 4B). The strongest MPP1 staining was observed in cells with bright mitosin-labelling, indicating enhanced MPP1 expression in G2. Accordingly, FACS analysis indicated a two to three fold increase of MPP1 expression as cells progress from G1 to G2/M (Fig 4B). During mitosis, in both prophase and metaphase cells, MPP1 staining showed fine punctuations diffuse throughout the cytoplasm (Fig 4C). At anaphase, MPP1 staining accumulated at the mid-plan of the cell and formed a distinct band extending across the spindle midzone (Fig 4C). In telophase cells, MPP1 was sharply concentrated in the midbody (Fig 4C).

We further used GFP-tagged MPP1 to visualize the dynamics of MPP1re-distribution during the cell cycle (Fig 5). We observed extensive cell death during establishment of the cell line, suggesting a toxic effect of MPP1 overexpression. In cells with a GFP-MPP1 level apparently similar to that of the endogenous protein (Figure 5A), the pattern of expression was similar to that of the endogenous protein (data not shown). During cytokinesis, time lapse imaging of GFP-tagged MPP1 showed MPP1 in the midbody first as a single spot and then as two dots, four dots and again as two spots. MPP1 concentration at the midbody then decreases asymetricaly, with a spot staying visible in only one of the daughter cell until abscission occurs (Fig 5B). This behavior suggests that the plus-end directed motor activity of MPP1 may play a role in MTs organization during cytokinesis exit.

Knockdown of MPP1 induces apoptosis and cytokinesis defects

We used small interfering RNA (siRNA) duplexes (37) to assess the consequences of MPP1 suppression (Fig 6 and 7). Human HCT116 epithelial cells were transfected with two independent MPP1-specific siRNAs. Results were similar with both siRNAs and are shown in the case of siRNA1 in Figures 6 and 7. Immunoblot analysis of cell extracts showed extensive depletion of MPP1 24 hours after transfection (Fig 6A). FACS analysis showed no clear modification at this time point, but after 48h, a hypodiploid peak appeared, indicating accumulation of apoptotic cells. Cell apoptosis was further enhanced at the point 72 hours following transfection with specific MPP1 oligoduplexes (Fig 6B). We then used phasecontrast videomicroscopy to examine the behavior of the cells over 36h duration, starting 18 hours after transfection (Fig 7). Over this period of time, most cells, which have lost MPP1 (Fig 7C), underwent at least one M-phase (Fig 7A). In MPP1-siRNA1 treated

cells, a high proportion of cytokinesis failure was observed (Fig 7A and B). Although a midbody formed, abscission did not occur. Either the midbody regressed with appearance of a binucleated cell, which further underwent apoptosis during a second round of mitosis or the midbody persisted and the two ill separated daughter cells finally underwent apoptosis. Such behaviour was observed in 42 % of siRNA treated cells whereas less than 10% control cells showed similar cytokinesis defects.

These data indicate that MPP1 is important for cell growth and completion of cytokinesis. Whereas it does not appear to be necessary for initiation of furrowing and cleavage furrow ingression it seems to play an important function for further cell separation.

Discussion

In this study, we find that MPP1, a member of a set of mitotic phosphoproteins specifically recognized by the MPM2 antibody at the G2/M transition (1), is a slow plus-end directed KRP that plays critical roles in cytokinesis.

As other KRPs, MPP1 exhibits MT activated-ATPase activity and binds to MTs (43). Additionally, MPP1 apparently bundles microtubules in vitro and behaves as a slow molecular motor in gliding assays. Phylogenic analysis of KRP motor domains (FP, unpublished results, (45,46)) shows that MPP1 belongs to the N6-class of KRPs, which includes RB6K (18,47,48) and orthologs of MKLP1 (49–52). As these KRPs, MPP1 displays an insertion in the N1–N2 sequence landmark of the motor domain when compared with conventional KHC (53). MPP1 insertion (77 aa) is the longest and this determines a N1–N2 spacing of 190 aa compared to less than 132 in other KRPs classes (53). MPP1 also displays an insertion (28 aa) at the end of the core motor domain, suggesting an extended neck linker region in the protein. Both MKLP1 and RB6K display similar insertions. Interestingly, motor domain and neck linker insertions concern loops (L6 and neck linker loop, respectively) whose interaction is important for motility behaviour (54) and this suggests concerted evolution of the two loop domains. As MPP1, MKLP1 cross-bridges microtubules in vitro and induces a slow (0.066 μm/s) plus-end movement of the tubulin polymers in gliding assays (50). These common functional features may be related to the structural characteristics shared by the two proteins.

MPP1 has a specific pattern of localization and expression during the cell cycle, being mostly nuclear in interphase cells with a sharp increase in expression in G2, diffuse in metaphase cells, with subsequent association to the central spindle and the midbody, at the end of mitosis. Motors with mitotic functions show similar cell-cycle regulated localization on mitotic structures and subsequent concentration in the midbody during cytokinesis (18,48,50,55–57). The midbody localization of MPP1 was not evident in previous works (46,58) but seems to be a consistent property of MPP1 in different localization assays (IF, GFP-MPP1 distribution in vivo) and different cell lines, HeLa, HCT116 (this work) and HUVEC (data not shown). This new localization of MPP1 seems important in light of our siRNA studies indicating a vital role of the protein in the correct completion of cytokinesis.

Cytokinesis depends on the presence of a number of proteins (59–61) including the other N6-class KRPs, RB6K and MKLP1 orthologs (18 ,19,48,49,51). Given their properties in vitro, these KRPs may be involved in both midzone microtubule bundling and subsequent microtubule sliding that are required for successful completion of cell cleavage (62). It is remarkable that MPP1, RB6K and MKLP1 are all independently required for cytokinesis, despite apparent functional and structural redundancy. Maybe, the rational for this multiplicity of motors will be revealed by detailed studies of molecular interactions between these motors themselves and between these motors and other major components of the midbody such as INCENP (63), survivin (64,65), TD60 (66), PRC1 (67). The three motors may also be included in different signalling pathways, involving different GTPases (68–71) and kinases (72–74).

In conclusion, our data show that MPP1 is a novel KRP whose activity is required for proper progression of cytokinesis in human cells. Further work is needed to see if this newly discovered function of MPP1 is related to its mitotic hyperphosphorylation.

Ackowledgements:

The authors thank D. Job for helpful discussion and comments during the writing of the manuscript. We are grateful to R. Cross, B. Goud and M. Bornens for their support. We are indebted to D. Grunwald and V. Collin for assistance with confocal microscopy and FACS. This work was supported by grants from LNCC (Ligue nationale contre le cancer, N° 10V04) and from ARC (Association pour la recherche contre le cancer, N° 9857) to F. Pirollet. J.M. Westendorf was supported by fellowships from ARC and FRM (Fondation pour la recherche médicale). A. Abaza was a recipient of French Research Ministry and a FRM fellowship.

Footnotes:

1

The abbreviations used are: MPF, M-phase promoting factor; MAPs: Microtubule-Associated Proteins; KRPs, Kinesin-related proteins; MTs, Microtubules; MPP1, M-phase phosphoprotein 1; GFP, Green fluorescent protein; siRNA, small interfering RNA.

References:

- 1. Matsumoto-Taniura N , Pirollet F , Monroe R , Gerace L , Westendorf JM 1996; Mol Biol Cell. 7: 1455- 1469
- 2. Dustin PD 1984; Microtubules. 2 Springer-Verlag; Berlin Heidelberg
- 3. Kirschner M , Mitchison T 1986; Cell. 45: 329- 342
- 4. Murray AW , Kirschner MW 1989; Science. 246: 614- 621
- 5. Lamb NJ , Fernandez A , Watrin A , Labbe JC , Cavadore JC 1990; Cell. 60: 151- 165
- 6. Morgan DO 1997; Annu Rev Cell Dev Biol. 13: 261- 291
- 7. O'Farrell PH 2001; Trends Cell Biol. 11: 512- 519
- 8. Burke B , Ellenberg J 2002; Nat Rev Mol Cell Biol. 3: 487- 497
- 9. Lowe M , Gonatas NK , Warren G 2000; J Cell Biol. 149: 341- 356
- 10. Hyman AA , Karsenti E 1996; Cell. 84: 401- 410
- 11. McNally FJ 1996; Curr Opin Cell Biol. 8: 23- 29
- 12. Heald R 2000; Nat Cell Biol. 2: E11- 12
- 13. Andersen SS 1999; Bioessays. 21: 53- 60
- 14. Valiron O , Caudron N , Job D 2001; Cell Mol Life Sci. 58: 2069- 2084
- 15. Hirokawa N , Noda Y , Okada Y 1998; Curr Opin Cell Biol. 10: 60- 73
- 16. Maney T , Hunter AW , Wagenbach M , Wordeman L 1998; J Cell Biol. 142: 787- 801
- 17. Blangy A , Lane HA , d'Herin P , Harper M , Kress M , Nigg EA 1995; Cell. 83: 1159- 1169
- 18. Fontijn RD , Goud B , Echard A , Jollivet F , van Marle J , Pannekoek H , Horrevoets AJ 2001; Mol Cell Biol. 21: 2944- 2955
- 19. Matuliene J , Kuriyama R 2002; Mol Biol Cell. 13: 1832- 1845
- 20. Verde F , Labbe JC , Doree M , Karsenti E 1990; Nature. 343: 233- 238
- 21. Ookata K , Hisanaga S , Sugita M , Okuyama A , Murofushi H , Kitazawa H , Chari S , Bulinski JC , Kishimoto T 1997; Biochemistry. 36: 15873- 15883
- 22. Ookata K , Hisanaga S , Bulinski JC , Murofushi H , Aizawa H , Itoh TJ , Hotani H , Okumura E , Tachibana K , Kishimoto T 1995; J Cell Biol. 128: 849- 862
- 23. Melander Gradin H , Marklund U , Larsson N , Chatila TA , Gullberg M 1997; Mol Cell Biol. 17: 3459- 3467
- 24. Westendorf JM , Rao PN , Gerace L 1994; Proc Natl Acad Sci U S A. 91: 714- 718
- 25. Davis FM , Tsao TY , Fowler SK , Rao PN 1983; Proc Natl Acad Sci U S A. 80: 2926- 2930
- 26. Davis FM , Rao PN Editor: Schlegel RA , Halleck MS , Rao PN 1987; Molecular regulation of nuclear events in mitosis and meiosis. 259- 293 Academic Press;
- 27. Sambrook J , Fritsch EF , Maniatis T 1989; Molecular cloning: a laboratory manual. 2 Cold Spring Harbor Lab. Press;
- 28. Mitchison T , Kirschner M 1984; Nature. 312: 232- 237
- 29. Desai A , Verma S , Mitchison TJ , Walczak CE 1999; Cell. 96: 69- 78
- 30. Pirollet F , Job D , Margolis RL , Garel JR 1987; Embo J. 6: 3247- 3252
- 31. Paturle-Lafanechère L , Manier M , Trigault N , Pirollet F , Mazarguil H , Job D 1994; J Cell Sci. 107: 1529- 1543
- 32. Huang TG , Hackney DD 1994; J Biol Chem. 269: 16493- 16501
- 33. Kapoor TM , Mitchison TJ 1999; Proc Natl Acad Sci U S A. 96: 9106- 9111
- 34. Condreay JP , Witherspoon SM , Clay WC , Kost TA 1999; Proc Natl Acad Sci U S A. 96: 127- 132
- 35. Harborth J , Elbashir SM , Bechert K , Tuschl T , Weber K 2001; J Cell Sci. 114: 4557- 4565
- 36. Chevrier V , Piel M , Collomb N , Saoudi Y , Frank R , Paintrand M , Narumiya S , Bornens M , Job D 2002; J Cell Biol. 157: 807- 817
- 37. Elbashir SM , Harborth J , Lendeckel W , Yalcin A , Weber K , Tuschl T 2001; Nature. 411: 494- 498
- 38. Savino TM , Gebrane-Younes J , De Mey J , Sibarita JB , Hernandez-Verdun D 2001; J Cell Biol. 153: 1097- 1110
- 39. Kozielski F , Sack S , Marx A , Thormahlen M , Schonbrunn E , Biou V , Thompson A , Mandelkow EM , Mandelkow E 1997; Cell. 91: 985- 994
- 40. Kull FJ , Sablin EP , Lau R , Fletterick RJ , Vale RD 1996; Nature. 380: 550- 555
- 41. Vale RD , Fletterick RJ 1997; Annu Rev Cell Dev Biol. 13: 745- 777
- 42. Lockhart A , Crevel IM , Cross RA 1995; J Mol Biol. 249: 763- 771
- 43. Woehlke G , Schliwa M 2000; Nat Rev Mol Cell Biol. 1: 50- 58
- 44. Zhu X , Mancini MA , Chang KH , Liu CY , Chen CF , Shan B , Jones D , Yang-Feng TL , Lee WH 1995; Mol Cell Biol. 15: 5017- 5029
- 45. Miki H , Setou M , Kaneshiro K , Hirokawa N 2001; Proc Natl Acad Sci U S A. 98: 7004- 7011
- 46. Kamimoto T , Zama T , Aoki R , Muro Y , Hagiwara M 2001; J Biol Chem. 276: 37520- 37528
- 47. Echard A , Jollivet F , Martinez O , Lacapere JJ , Rousselet A , Janoueix-Lerosey I , Goud B 1998; Science. 279: 580- 585
- 48. Hill E , Clarke M , Barr FA 2000; Embo J. 19: 5711- 5719
- 49. Adams RR , Tavares AA , Salzberg A , Bellen HJ , Glover DM 1998; Genes Dev. 12: 1483- 1494
- 50. Nislow C , Lombillo VA , Kuriyama R , McIntosh JR 1992; Nature. 359: 543- 547
- 51. Raich WB , Moran AN , Rothman JH , Hardin J 1998; Mol Biol Cell. 9: 2037- 2049
- 52. Kuriyama R , Dragas-Granoic S , Maekawa T , Vassilev A , Khodjakov A , Kobayashi H 1994; J Cell Sci. 107: 3485- 3499
- 53. Wade RH 2002; Structure (Camb). 10: 1329- 1336
- 54. Wade RH , Kozielski F 2000; Nat Struct Biol. 7: 456- 460
- 55. Yen TJ , Li G , Schaar BT , Szilak I , Cleveland DW 1992; Nature. 359: 536- 539
- 56. Wordeman L , Mitchison TJ 1995; J Cell Biol. 128: 95- 104
- 57. Vernos I , Raats J , Hirano T , Heasman J , Karsenti E , Wylie C 1995; Cell. 81: 117- 127
- 58. Fritzler MJ , Kerfoot SM , Feasby TE , Zochodne DW , Westendorf JM , Dalmau JO , Chan EK 2000; J Investig Med. 48: 28- 39
- 59. Robinson DN , Spudich JA 2000; Trends Cell Biol. 10: 228- 237
- 60. Glotzer M 2001; Annu Rev Cell Dev Biol. 17: 351- 386
- 61. Somma MP , Fasulo B , Cenci G , Cundari E , Gatti M 2002; Mol Biol Cell. 13: 2448- 2460
- 62. Wheatley SP , Wang Y 1996; J Cell Biol. 135: 981- 989
- 63. Mackay AM , Ainsztein AM , Eckley DM , Earnshaw WC 1998; J Cell Biol. 140: 991- 1002
- 64. Li F , Ackermann EJ , Bennett CF , Rothermel AL , Plescia J , Tognin S , Villa A , Marchisio PC , Altieri DC 1999; Nat Cell Biol. 1: 461- 466
- 65. Chen J , Wu W , Tahir SK , Kroeger PE , Rosenberg SH , Cowsert LM , Bennett F , Krajewski S , Krajewska M , Welsh K , Reed JC , Ng SC 2000; Neoplasia. 2: 235- 241
- 66. Martineau-Thuillier S , Andreassen PR , Margolis RL 1998; Chromosoma. 107: 461- 470
- 67. Mollinari C , Kleman JP , Jiang W , Schoehn G , Hunter T , Margolis RL 2002; J Cell Biol. 157: 1175- 1186
- 68. Boman AL , Kuai J , Zhu X , Chen J , Kuriyama R , Kahn RA 1999; Cell Motil Cytoskeleton. 44: 119- 132
- 69. Jantsch-Plunger V , Gönczy P , Romano A , Schnabel H , Hamill D , Schnabel R , Hyman AA , Glotzer M 2000; J Cell Biol. 149: 1391- 1404

- 70. Tatsumoto T , Xie X , Blumenthal R , Okamoto I , Miki T 1999; J Cell Biol. 147: 921- 928
- 71. Hirose K , Kawashima T , Iwamoto I , Nosaka T , Kitamura T 2001; J Biol Chem. 276: 5821- 5828
- 72. Terada Y , Tatsuka M , Suzuki F , Yasuda Y , Fujita S , Otsu M 1998; Embo J. 17: 667- 676
- 73. Severson AF , Hamill DR , Carter JC , Schumacher J , Bowerman B 2000; Curr Biol. 10: 1162- 1171
- 74. Lee KS , Yuan YL , Kuriyama R , Erikson RL 1995; Mol Cell Biol. 15: 7143- 7151
- 75. Lupas A , Van Dyke M , Stock J 1991; Science. 252: 1162- 1164
- 76. Cokol M , Nair R , Rost B 2000; EMBO Rep. 1: 411- 415
- 77. Wiemann S , Weil B , Wellenreuther R , Gassenhuber J , Glassl S , Ansorge W , Bocher M , Blocker H , Bauersachs S , Blum H , Lauber J , Dusterhoft A , Beyer A , Kohrer K , Strack N , Mewes HW , Ottenwalder B , Obermaier B , Tampe J , Heubner D , Wambutt R , Korn B , Klein M , Poustka A 2001; Genome Res. 11: 422- 435
- 78. Sablin EP , Kull FJ , Cooke R , Vale RD , Fletterick RJ 1996; Nature. 380: 555- 559
- 79. Endow SA 1999; Nat Cell Biol. 1: E163- 167

Fig. 1

Structural organization of human MPP1

A. Human MPP1 cDNA representation and genomic organization. The three cDNAs 6-1, 1L9 and 1C12 that were cloned as detailed under Experimental procedures are drawn as thin lines above the schematic representation of the full-length MPP1 cDNA. Horizontal lines indicate 5′ and 3′-untranslated regions. The enlarged 70–5412 sequence encodes a kinesin family member, 1,780 amino acid residues long whose predictive mass is 206,187. It exhibits a conserved organization into three regions (15). The dark grey box (M), which corresponds to the hyper-conserved motor domain, indicates that MPP1 is an NH2-terminal motor. In the central region, four α-helical domains (C1 to C4) shown in light grey are predicted to form coiled-coil conformations as determined by the program of Lupas et al (75). The tail region, which is supposed to interact with cargos, exhibits five putative MPM2-recognition sites and one presumptive NLS as indicated with grey and black triangles (24,76). No putative PEST and cyclin or DNA-binding domains sequences were found. HsMPP1 is identical to the recently described KRMP1 found independently by another laboratory and the hypothetical protein CAB55962, with the exception of 9 and 2 aa, respectively (46,77). The very high sequence identity suggests that the same gene encodes them all. The human genomic MPP1 locus (gb AL 157389) was identified using the MPP1 cDNA as a query in the Blast algorithm against the human genome database. The intron-exon boundaries were defined by direct comparison of the cDNA sequence against the genomic sequence. The corresponding exonintron structure of the human MPP1 gene is shown below with exons as numbered boxes and introns as connecting lines. B. Comparison of MPP1 and conventional KHC motor domains. Sequences of the first 550 and 350 amino acids of MPP1 and HsuKHC (sp P33176) were aligned using the Blast 2 sequences program. Sequences are 40% similar with 25% identity. Conserved residues are in bold and the positions of secondary structure elements are indicated according to KHC crystallographic data (39,40). The four conserved motifs, which interact with ATP, are drawn as boxes N1–4 as defined by Sablin et al (78). The open triangle indicates the limit between the KHC motor core domain and its neck region, which consists of β9 and β10 strands and a weak coiled-coil region extending at aa 352 (79). The heptad repeat positions predicted by Coils are underlined.

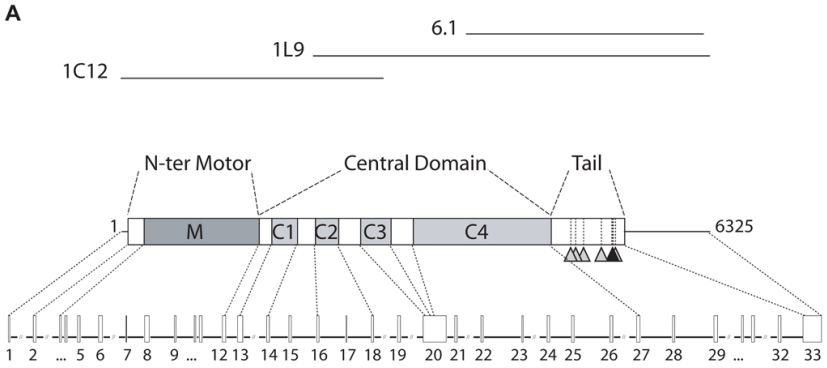

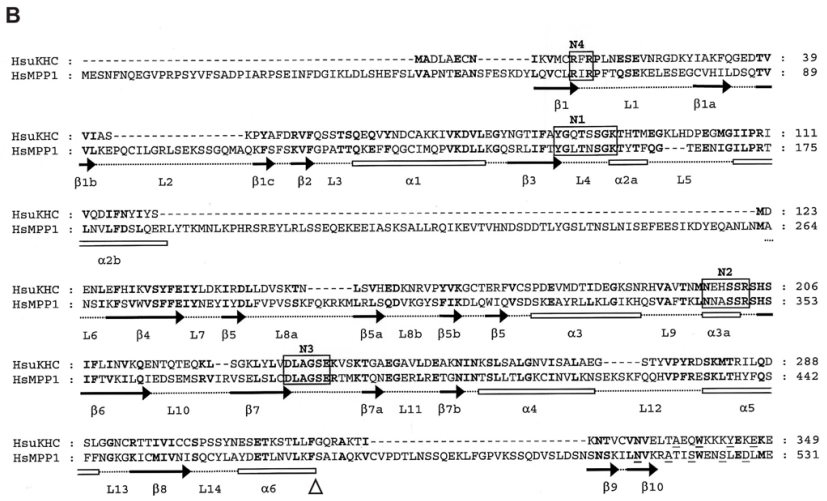

Fig. 2

Purification of recombinant MPP1 mutants and immunoblot analysis of MPP1 distribution in various human tissues

A. Preparation of recombinant full-length protein and MC1 mutant. Recombinant full-length MPP1 protein, rMPP1, or the deletion mutant rMC1 (aa 1–650), which contains the putative motor domain and the first α-helical domain C1, were synthesized as FLAG-tagged fusion proteins and purified to near homogeneity from insect cells as described under Experimental procedures. They were run on an 8% PAGE-SDS gel and stained by Coomassie. rMPP1 migration corresponds to the predicted size of MPP1 and to its previously identified apparent molecular mass (1). On the other hand, rMC1 migrates anomalously large with an apparent MW ~15 kDa larger than MW calculated, suggesting an elongated form of the mutant. A schematic representation of the two constructs is drawn. B. Immunoblot of recombinant MPP1 mutants and of various human cell and tissues extracts. Tissue homogenates were aliquots of Clontech's human protein medleys. Recombinant proteins (10 ng) or extracts (20 μg) were run on 8% PAGE-SDS gel, transferred to Immobilon P (Amersham) in the presence of 0.01% SDS and immunoreacted with an affinity-purified anti-MPP1 antibody (0.5 μg/ml) prepared as described under Experimental procedures. ECL substrat (Amersham) was used for detection. Lack of reactivity with rMC1 mutant indicates that we selected antibodies, which recognize epitopes present in the C2 to tail domains, the most specific portion of the protein when compared to other KLPs.

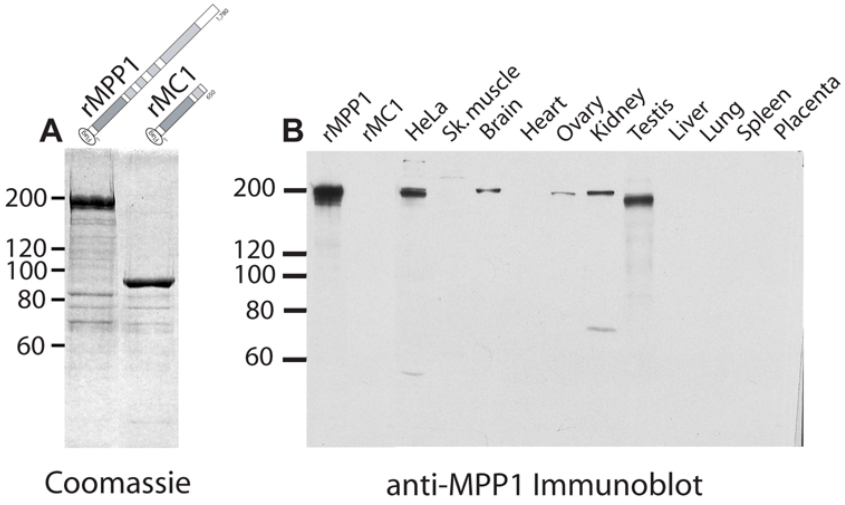

Fig. 3

Activity of recombinant MPP1 and MC1

A. MT-activated ATPase activity. ATPase activities of the two fragments were assayed as described under Experimental procedures. Reactions were started by addition of the protein, 25 nM rMPP1 or 66 nM rMC1. $K_{1/2\ MT}$ was measured in presence of 2 mM Mg- ATP, using MT ranging from 0.1 to 10 μM and maximum k_{cat} was indicated. Km for ATP was determined in presence of 2 μM taxol-stabilized MTs, using Mg-ATP concentrations ranging from 0.025 to 4 mM. A similar assay using 250 nM MPP1 or 320 nM MC1 with 2 mM ATP in absence of MTs allowed measuring of MT-independent basal ATPase activity. Data represent the results from the two best motor preparations and mean values are shown with the SEM. B. Nucleotide-dependent promotion of MT bundling in vitro. rMPP1 and rMC1 were incubated with taxol-stabilized MTs in the presence or in the absence of ATP. The reactions were diluted in a fixative medium and sedimented onto glass coverslips. Tubulin and recombinant fragments were stained with specific antibodies. The upper panels show the distribution of MTs, lower ones the distribution of MPP1 mutants. Bar = 20 μm. C. rMC1 moves MTs with their minus end leading. Four frames from a time lapse fluorescence microscopy video of a rMC1-gliding assay using polarity-marked MTs at 30°C are shown. The starting position of the – end of the MT is indicated by the white arrowhead. Bar = 6 μm

A

	$K_{1/2\ MT}$ (μM)	k_{cat} (s^{-1})	Km ATP (mM)	Basal k_{cat} (s^{-1})
rMPP1	0.72 ± 0.23	7.73 ± 0.34	0.21 ± 0.02	0.027
rMC1	4.43 ± 0.20	10.18 ± 1.96	0.24 ± 0.01	0.016

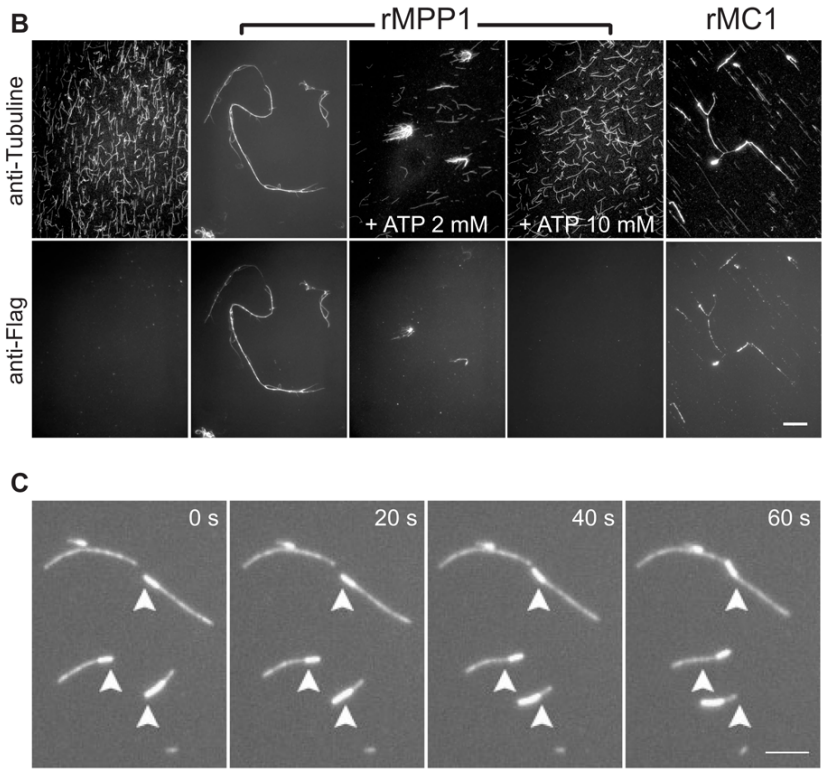

Fig. 4

Cell-cycle regulated MPP1 expression

A. MPP1 localizes mainly to the interphasic nuclei. HeLa cells were stained with the anti-MPP1 antibody (left panel) and an anti-β-tubulin monoclonal antibody (right panel) as described under Experimental procedures. Z Projections of confocal images are shown. Bar = 20 μm. B. MPP1 expression is increased in G2/M cells. Upper panels show confocal images of indirect immunofluorescence of HeLa cells stained with the anti-MPP1 (left) and antimitosin (right) antibodies. Lower panels show FACS analysis of HeLa cells stained with the same antibodies together with Hoechst and processed as described under Experimental procedures. C. MPP1 localizes to mitotic structures. HeLa cells were stained with the anti-MPP1 antibody (left panel) and anti-β-tubulin antibody (right panel) as in A.

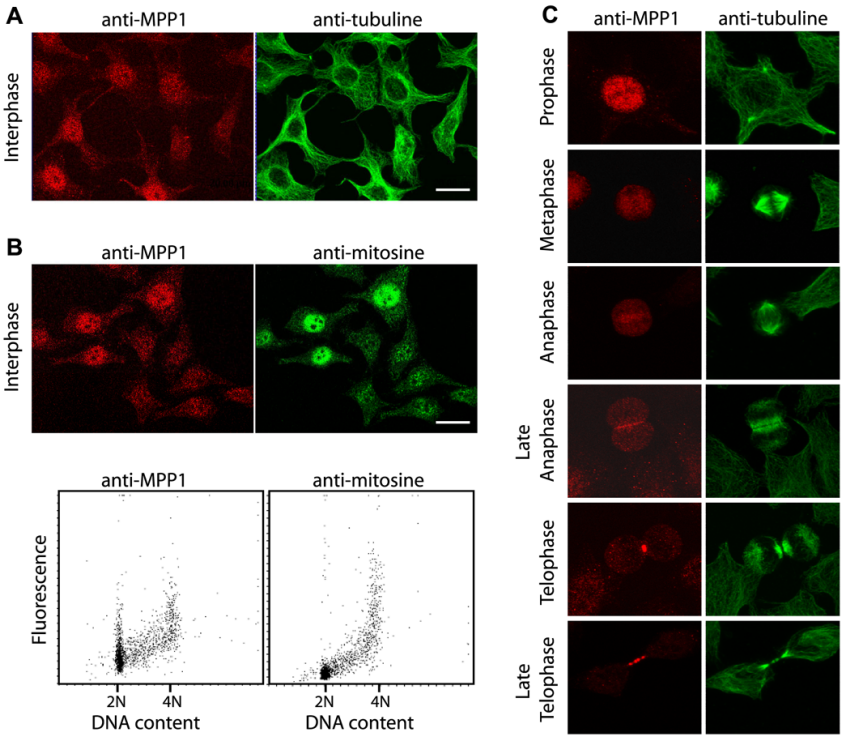

Fig. 5

Ectopic GFP-MPP1 localizes to the midbody

A. Level of GFP-MPP1 expression in a stable HeLa cell line. HeLa cells were stably transfected with a GFP-MPP1 construct as described under Experimental procedures. Similar amounts of untransfected (left lanes) or stably transfected cells (right lanes) were harvested and either boiled into SDS-PAGE sample buffer (upper panel) or immunoprecipitated (lower panel) with monoclonal anti-GFP antibodies (Boehringer Mannheim) as described by the manufacturer. Extracts were then analysed by immunoblot with the anti-MPP1 antibody. The signals of both MPP1 and GFP-MPP1 fusion protein that migrates at the predicted higher apparent MW are similar, indicating that the two proteins have similar levels of expression. B. Localization of exogenous GFP-MPP1 during cytokinesis. A telophasic cell was searched in the layer of GFP-MPP1 HeLa cells and time-lapse Z-sequences were collected and analyzed as described under Experimental procedures. As a rule 30 sequential Z-axis fluorescent images were collected in 0.3 μm steps, every 3 min. Selected frames of the timelapse epifluorescence microscopy videos were shown. Time for elongation and break of the midbody is indicated in min.

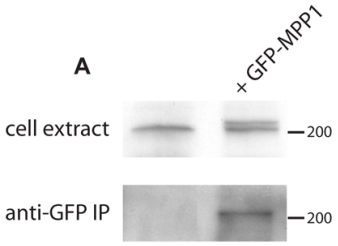

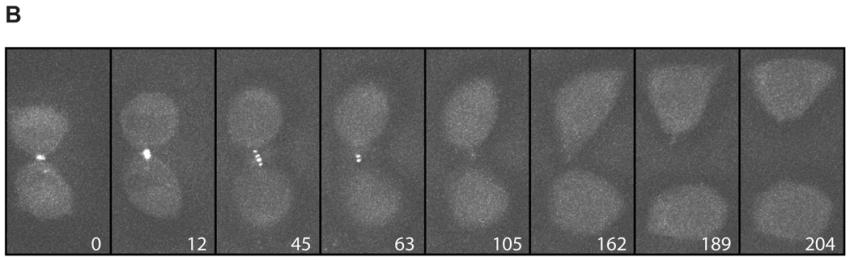

Fig. 6

MPP1-depleted cells undergo cell death

A. Reduction of MPP1 levels after MPP1-specific siRNA transfection. HCT116 cells were transfected with buffer (Bu) or with siRNA homologous (siRNA1) or not homologous (siRNA1m or U) to MPP1, as described under Experimental procedures. Cells were harvested 24 h after transfection and subjected to immunoblot analysis with the anti-MPP1 antibody. siRNAs used are indicated above each lane. Specific targeting of MPP1 was demonstrated by the lack of reduction observed after use of mutated or unrelated sequences as well as buffer instead of the volume of siRNA1. Reprobing of the blot with an anti-tubulin antibody confirm equal loading of the samples (data not shown). B. Time course of change in cellular DNA content after siRNA transfection. Cells were transfected as above and analyzed by flow cytometry as described under Experimental procedures. Time after transfection (T) is in hours. Best results from three independently performed experiments are shown.

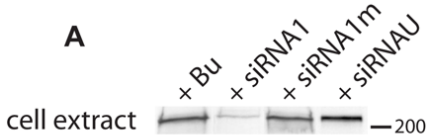

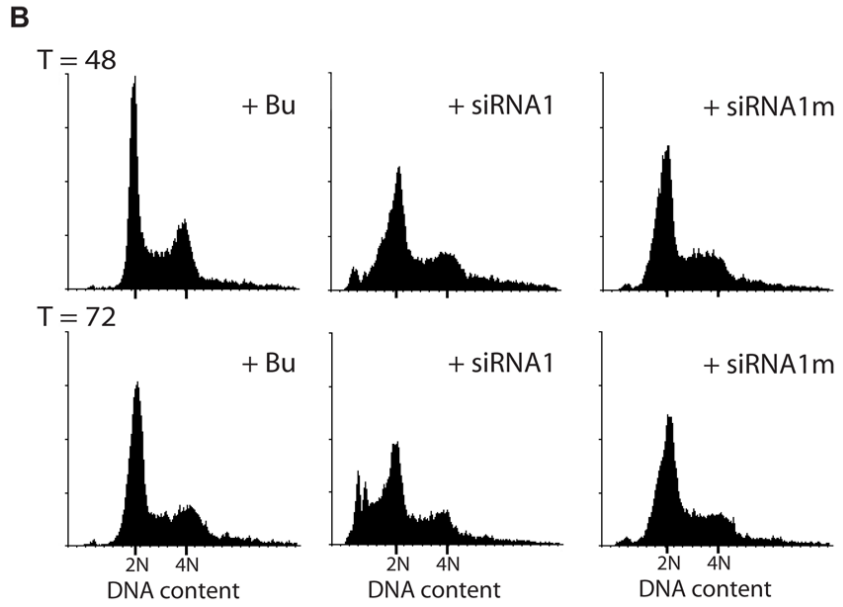

Fig. 7

MPP1-depleted cells exhibit mitotic defects

A. Quantitation of cell progression phenotypes of control and MPP1-siRNA transfected cells. HCT116 cells were transfected as in Figure 6, transferred to live-cells chambers and three different fields were imaged every 5 min as described under Experimental procedures. Fifty to 60 cells were picked up randomly on the three images taken 18h after transfection and were followed until 54 h after transfection. HCT116 cells were scored for the various phenotypes observed in their cell cycle progression. When cells were dense, blebbing, with non-uniform membranes they were scored as apoptotic. Most of the cells become rounded and a well formed midbody between the two daughter cells appeared indicating that they were undergoing mitosis. When two viable daughter cells were formed, the cells were scored as going through successful mitosis. However, various defects in mitotic exit, daughter cells separation and further appearance of apoptosis were sometimes observed and the cells were then scored as undergoing failure of mitosis. In other cases, either mitosis or apoptosis were observed and we hypothesize that cells may be blocked. B. Cell cycle progression of control and MPP1-siRNA transfected cells. Selected frames of the time-lapse phase-contrast microscopy videos were shown: top row after transfection with siRNAU duplex, one typical control siRNA-transfected cell; middle and bottom rows after transfection with specific siRNA1 duplex, two typical siRNA1-transfected cells undergoing mitosis failure. The black arrow indicates the cell observed. m1 and m2 indicate entry into first or second mitosis, daughter cells are labelled with white arrows. Symbol marks (
, ★) show daughter cells from the same mitotic cell. md indicates a mitotic defect, bin, a binucleated cell and a, an apoptotic cell. Time shown is in hours and min. C. MPP1 expression in siRNA-transfected cells. Indirect immunofluorescence of HCT116 cells stained with the anti-MPP1 antibody, 24 h after transfection with the indicated duplexes. The pattern obtained after siRNAU transfection is similar to the one after mockand siRNAi1m transfection (data not shown). As the cells were stained and the pictures acquired and processed under exactly the same conditions, this indicates that the level of transfection with siRNAi1 was very high and we can assume that the cells that we looked at in Fig 7B are actually transfected.